DOCUMENT RESUME

ED 259 945 SE 045 922

AUTHOR	Nordmark, Staffan
TITLE	VTI Driving Simulator: Mathematical Model of a Four-wheeled Vehicle for Simulation in Real Time. VTI Rapport 267A.
INSTITUTION	Swedish Road and Traffic Research Inst., Linkoping.
REPORT NO	VTI-R-267A-1984
PUB DATE	84
NOTE	69p.
AVAILABLE FROM	Swedish Road and Traffic Research Inst., S-581 01, Linkoping, Sweden.
PUB TYPE	Reports - Descriptive (141) -- Collected Works - Serials (022)
JOURNAL CIT	VTI Rapport; n267A 1984
EDRS PRICE	MF01 Plus Postage. PC Not Available from EDRS.
DESCRIPTORS	*Computer Simulation; Computer Software; *Driver Education; Foreign Countries; *Mathematical Models; *Motor Vehicles; Simulation
IDENTIFIERS	*Driving Simulators; Sweden

ABSTRACT

This report contains a theoretical model for describing the motion of a passenger car. The simulation program based on this model is used in conjunction with an advanced driving simulator and run in real time. The mathematical model is complete in the sense that the dynamics of the engine, transmission and steering system is described in some detail. Tire forces are given by tabular data. Steering and suspension compliances are lumped together with the tire forces to give effective cornering characteristics. Wheel rotational equations are integrated and the associated difficulties discussed. Rolling resistance and aerodynamic forces are included to some extent. The model is validated during transient manoeuvers and the results correspond well with field test data. (Author)

****
* Reproductions supplied by EDRS are the best that can be made *
* from the original document. *
****

Klintland Grafiska, Linköping 1964

CONTENTS

		Page
ABSTRACT		I
REFERAT		II
SUMMARY		III
SAMMANFATTNING		VI
1	INTRODUCTION	1
2	MODEL DESCRIPTION	5
3	COORDINATE SYSTEMS AND TRANSFORMATIONS	6
4	EQUATIONS OF MOTION	7
5	EXTERNAL FORCES	9
6	WHEEL DYNAMICS	13
7	TIRES AND SUSPENSIONS	19
7.1	Tire model	19
7.2	Aligning torque. Free rolling wheel	22
7.3	Suspension and steering compliances. Effective cornering characteristics	25
7.4	Tire carcass elasticity	28
8	BRAKING SYSTEM	31
9	ENGINE AND DRIVE LINE	33
10	STEERING SYSTEM	38
11	ROLLING RESISTANCE AND WIND FORCES	42
12	VALIDATION	45
REFERENCES		51
LIST OF SYMBOLS		53

VTI DRIVING SIMULATOR - Mathematical Model of a Four-wheeled Vehicle for Simulation in Real Time

by Staffan Nordmark
Swedish Road and Traffic Research Institute
S-581 01 LINKÖPING Sweden

ABSTRACT

This report contains a theoretical model for describing the motion of a passenger car. The simulation program based on this model is used in conjunction with an advanced driving simulator and run in real time. The mathematical model is complete in the sense that the dynamics of the engine, transmission and steering system is described in some detail. Tire forces are given by tabular data. Steering and suspension compliances are lumped together with the tire forces to give effective cornering characteristics. Wheel rotational equations are integrated and the associated difficulties discussed. Rolling resistance and aerodynamic forces are included to some extent. The model is validated during transient manoeuvres and the results correspond well with field test data.

VTI KÖRSIMULATOR - Matematisk modell av ett fyrhjuligt fordon för realtidssimulering

av Staffan Nordmark
Statens väg- och trafikinstitut
581 01 LINKÖPING

REFERAT

Denna rapport innehåller en teoretisk modell som beskriver en bils rörelse. Det simuleringsprogram, som grundar sig på denna modell, används i en avancerad körsimulator och körs alltså i realtid. Den matematiska modellen beskriver även motorns, transmissionens och styrningens egenskaper detaljerat. Däckskrafterna ges av tabellerade värden. Styrningens och hjulupphängningens elasticiteter kopplas ihop med däcket och ger en resulterande sidkraftkarakteristik. Hjulens rotationsekvationer integreras och svårigheterna därvid diskuteras. Rullmotstånd och luftkrafter är medtagna i viss utsträckning. Modellen är validerad under transienta manövrer och resultaten överensstämmer väl med fältexperiment.

VTI DRIVING SIMULATOR - Mathematical Model of a Four-wheeled Vehicle for Simulation in Real Time

by Staffan Nordmark
Swedish Road and Traffic Research Institute
S-581 01 LINKÖPING Sweden

SUMMARY

This report describes the mathematical model of a passenger car that is currently used in an advanced driving simulator at the Swedish Road and Traffic Research Institute.

The basic model describes a four-wheeled vehicle with freedom to move in the plane and to yaw. Neither roll nor pitch are included but a semistatic load transfer between the wheels is used. The distribution of this load transfer is specified among the input data thus obtaining some of the effects of different spring layouts. This is very important since the horizontal tire forces depend on the vertical load in a nonlinear manner.

The difficulties to integrate the rotational equations of motion for the wheels are discussed especially when the time-step is comparatively long. One approximate solution to this problem is described.

The horizontal tire forces are given as tabular data and depend on the vertical load, slip angle and longitudinal slip. Intermediate values are computed by linear interpolation and it is assumed that the functions can be factorized in a special way.

Simple analytical tire models have been tried, but these tend to give a coupling too strong between lateral and longitudinal forces. This will result in exaggerating the difference between front and rear driven cars.

It is not only the tire cornerning characteristics that determine the handling qualities of car. The suspensions and steering system will add compliance to the tires thus influencing the overall cornering stiffness. We have chosen to use the concept of effective cornering characteristics i. e. these compliances are lumped together with that of the tire. This procedure is described in detail.

Due to tire carcass elasticity the contact patch between tire and ground will move relatively the wheel center. This will induce torques on the vehicle mass as well as changes in steering angles and is in fact the main reason for the tendency of vehicles to tuck inwards a curve when the throttle is released. These effects are for that reason included in the model.

The braking system has as option a reduction valve coupled to the brakes of the rear wheels.

The engine and driveline are also described in some detail. A simple but effective algorithm is given for the complex relationship between throttle, engine torque and engine speed. The most important qualities of the final drive with differential is included dividing the torque equally between the wheels and coupling the moment of inertia of the flywheel to that of the wheels.

The reaction torque at the steering wheel is computed for small steer angles but the effects of inclinations of the steering axis are considered in detail. Some Coulomb damping is included and hysteresis effects is obtained by first order filtering of the damping.

Rolling resistance of the wheels are introduced at each wheel and aerodynamic drag proportional to the square of velocity is used to maximize the speed. Side wind

and wind gusts perpendicular to the vehicle trajectory are also given in equation form. These can be used as surprise elements to a driver in the simulator.

VTI KÖRSIMULATOR - Matematisk modell av ett fyrhjuligt fordon för realtidssimulering

av Staffan Nordmark
Statens väg- och trafikinstitut
581 01 LINKÖPING Sweden

SAMMANFATTNINC

Denna rapport beskriver det teoretiska underlaget till ett program som beskriver kördynamiken hos en personbil. Detta program används i en avancerad körsimulator som för närvarande är i bruk vid Statens väg- och trafikinstitut (VTI).

I princip beskrivs med ekvationer rörelsen hos ett fordon med fyra hjul som kan röra sig på ett plan i alla riktningar samt vrida sig runt en vertikalaxel (girrörelse). Varken kräng- eller tipprörelse beaktas men den lastöverflyttning mellan hjulen som sker p g a accelerationer är medräknad genom ett "semistatiskt" betraktelsesätt. Lastöverflyttningen i sidled fördelas mellan fram- och bakaxel i proportioner som anges som indata till programmet. På detta sätt kan olika val av krängstyvheter fram - bak simuleras. Detta är mycket viktigt eftersom de horisontella däckskrafterna i allmänhet är olinjära funktioner av vertikalbelastningen.

Svårigheterna då det gäller att integrera rotationsekvationerna för hjulen diskuteras och speciellt fallet med ett relativt sett långt tidssteg. En approximativ lösning till detta problem är angiven.

De horisontella däckskrafterna ges som tabellvärden och är funktioner av vertikalbelastning, avdriftsvinkel och longitudinellt slip. Mellanliggande värden beräknas med linjär interpolation och som förenkling

antas att funktionerna kan faktoriseras på ett speciellt sätt.

Enkla analytiska modeller för däckskrafterna har provats, men dessa tenderar att ha en alltför stark koppling mellan sid- och längskraft. Detta leder till att överdriva skillnaderna mellan fram- och bakhjulsdrivna bilar.

Det är inte bara däckens sidkraftkarakteristika som bestämmer ett fordons köregenskaper. Fjädersystemet och styrningen är ofta eftergivlig då man lägger på en sidkraft och påverkar på detta sätt den sammanlagda sidkraftskoefficienten. Vi har valt att arbeta med sådana resulterande sidkraftskarakteristika där dessa eftergivligheter adderas till däcket självt. Denna metod beskrivs i detalj.

På grund av däckets och framför allt däcksidans mjukhet kommer kontaktytan mellan däck och vägbana att förskjutas från en punkt under hjulcentrum. Detta gör att speciellt de longitudinella krafterna kommer att utöva ett (återställande) moment på fordonet under kurvtagning. Detta är den främsta orsaken till så kallade gas-släpp-reaktioner i kurva. Vidare kan dessa moment orsaka förändrade styrvinklar vilket påverkar beteendet under sådana manövrer. Av denna anledning är dessa effekter behandlade i modellen.

Bromssystemet är i huvudsak en proportionell överföring av pedalkraft till bromsmoment. Möjligheten av en tryckreduceringsventil till bakaxeln finns dock med.

Motorn och kraftöverföringen beskrivs ganska detaljerat. En enkel men användbar algoritm anges för det komplicerade sambandet mellan gaspådrag, vridmoment

och varvtal. De viktigaste egenskaperna hos differentialen finns med såsom att momentet fördelas lika mellan drivhjulen och att svänghjulets tröghetsmoment adderas till drivhjulens.

Reaktionsmomentet i ratten är beräknat för små styrvinklar men hänsyn har tagits till styraxlarnas lutning i olika riktningar. Coulomb-friktion är inlagt i styrsystemet och för att åstadkomma hysteres dämpas denna signal med ett första ordningens filter.

Rullmotstånd proportionellt mot vertikalbelastningen är inlagt vid varje hjul. Fordonets maximala hastighet begränsas av luftmotståndet som är proportionellt mot kvadraten på hastigheten. Likaså finns möjlighet att lägga in sidvind eller vindbyar rakt från sidan. Dessa kan användas som överraskningsmoment för en förare i simulatorn.

U.S. DEPARTMENT OF EDUCATION
NATIONAL INSTITUTE OF EDUCATION
EDUCATIONAL RESOURCES INFORMATION CENTER (ERIC)

☑ This document has been reproduced as received from the person or organization originating it.

☐ Minor changes have been made to improve reproduction quality.

• Points of view or opinions stated in this document do not necessarily represent official NIE position or policy.

"PERMISSION TO REPRODUCE THIS MATERIAL IN MICROFICHE ONLY HAS BEEN GRANTED BY

Birgitta Sandstedt

TO THE EDUCATIONAL RESOURCES INFORMATION CENTER (ERIC)."

1 INTRODUCTION

This report describes the mathematical model of a passenger car that is currently used in an advanced driving simulator at the Swedish Road and Traffic Research Institute (VTI).

The plans for building a simulator at VTI can be traced back to the sixties but first in 1978 the financial support from the National Swedish Board for Technical Development made it possible to build such a system. Different versions of the simulator have been in operation during these years. The development stages have spanned from only a chair and steering wheel standing on the floor with a simple oscilloscope picture to the moving base simulator with wide angle visual system that is used today. An important step in the development was taken during the spring 1983 when it was possible to drive the simulator with the complete moving base system for the first time. There is of course room for improvements and the development will continue.

The current version is equipped with a moving base system for simulating inertia forces. The design and general lay-out of the simulator is of course inspired by existing simulators elsewhere and most notably the one at VW-Werk. The VW-simulator [12] works with rotations of the cabin (roll, pitch and yaw) where the basic idea is to use a component of the gravitational acceleration to simulate accelerations in different directions. The VTI-system also has three degrees of freedom but the yaw motion has been cancelled in favour of pure lateral motion along rails. See figure 1.1.

The lateral inertia forces can thus be simulated both by giving the cabin a specified roll angle and by

lateral acceleration. These two principles are combined to use the roll mainly for constant accelerations as in a curve while lateral motion is used for manoeuvres on straight roads. The longitudinal accelerations are simulated only by giving the cabin a suitable pitch angle.

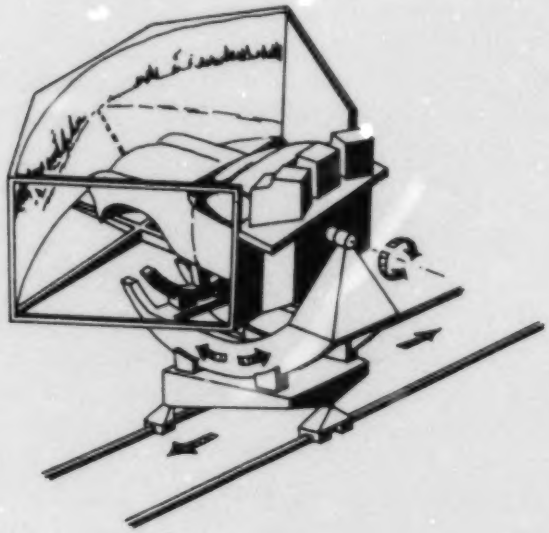

Figure 1.1 General lay-out of driving simulator with moving base system

All the motions are operated by hydraulic engines via chains and the hydraulic system is dimensioned for simulating accelerations up to 0.4 g. This means that some scaling of accelerations must be used when driving on high friction surfaces.

The vision field is produced by three colour TV-projectors mounted above the driver's head and the

screens are situated in front of the head at approximately a distance of two metres from the eyes of the driver. The road picture is generated purely by electronics developed at VTI and consists of different kinds of roads and surroundings. The horizontal and vertical curvature can be continuously varied and several objects (signs, obstacles etc) be introduced.

This report will describe in detail the mathematical model that is used for describing the vehicle and its motion. This is an out-growth of an earlier attempt described in [10]. That report was written to form a base for program construction at the initial development phase. At that time a hybrid computer was available and most parts of the model were successfully programmed.

The important friction forces between tires and ground were modelled by using simple analytical expressions as derived in [2]. Experiments in an early fixed-base simulator indicated a qualitatively correct behaviour of the vehicle but there was certainly room for improvements. Specially it was felt that traction and braking forces influenced the handling qualities too much and it was hard to obtain a normal degree of understeer without lowering the cornering stiffness at the front.

Based on these experiences a fairly large revision was carried out. The friction forces between tire and ground were now given in tabular form using linear interpolation and suspension and steering system compliances were included in the tire model by computing the effective cornering characteristics.

Since the program must run in real time there is a limit in model complexity determined by the available

computer and the time step used. We have chosen not to describe the vertical working of suspensions and sprung mass motion, but rather concentrate on the representation of tire forces and steering effects in suspensions. Comparisons with field test data have supported this approach. Very good agreement has been reached between field test data and results from the computer when studying the transient behaviour of a passenger car performing lane change manoeuvres with different severity and rapidness.

The program is written in FORTRAN 77 and run on a SEL 32/57. The cycle time (time available to exchange data between cabin and computer and run through the computer program once) is 20 ms and today is 12 ms used. This is valid for the complete program including parts governing the motion of the moving base system and the visual system besides the vehicle dynamics.

Naturally a simulation model is a mixture of parts from different sources. We have tried to state the origins of different ideas when possible. The people involved in this project have all contributed to this report to some extent. This is specially valid for Mats Lidström who has programmed several of the earlier versions of the simulator program. He has also constructed the very effective model of the engine characteristics.

2 MODEL DESCRIPTION

The vehicle is modelled as a stiff box with four wheels moving on a flat surface. Essentially this means a system with three degrees of freedom: linear motion in the plane and yaw. The sprung mass is neither allowed to roll nor pitch. However, load transfer between the wheels is used, in a semi-static fashion to simulate the effects of different suspension layouts.

The greatest effort has been spent to give a careful description of the friction forces between tire and ground. Compliances in the steering system and suspensions are considered as far as their influence on handling qualities are concerned.

For this model the following equations are given which are described in detail in the following sections

a) Equations of motion for the vehicle in the plane

b) Rotational dynamics of the wheels

c) Engine and driveline

d) Tire model giving horizontal forces and torques between tire and ground

e) Steering system

3 COORDINATE SYSTEMS AND TRANSFORMATIONS

In the sequel the following coordinate systems are used

a) (Q X Y Z) A groundfixed system with Z- axle pointing upward

b) (G x' y' z') A system with the axles parallell with (XYZ) and origin G in the centre of the vehicle

c) (G x y z) The system (Gx'y'z') rotated the angle ψ around the z'- axle.

For the transformation of a vector $\bar{a}$ between the systems b) and c) we have the following expression

$$(\bar{a}) = A(\bar{a})'$$

where A is the orthogonal transformation matrix

$$A = \begin{pmatrix} \cos\psi & \sin\psi & 0 \\ -\sin\psi & \cos\psi & 0 \\ 0 & 0 & 1 \end{pmatrix}$$

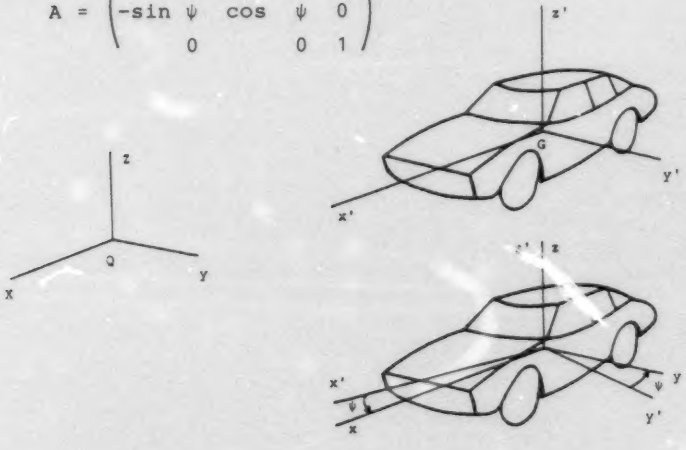

Figure 3.1 The orientation of the coordinate systems mentioned in section 3.

4 EQUATIONS OF MOTION

Written in vector form the equation for the planar motion of the vehicle centre of gravity is

$$m \ddot{\bar{x}} = \bar{F}_e \qquad (4.1)$$

It is natural to express this equation in the body fixed (G x y z)- system since the lateral and longitudinal speeds have an easy interpretation in this case.

The speed is thus

$$\dot{\bar{x}} = \begin{pmatrix} u \\ v \\ 0 \end{pmatrix}$$

in the (G x y z)- system which is rotating with the angular speed

$$\bar{\omega}_o = \begin{pmatrix} 0 \\ 0 \\ r \end{pmatrix}$$

The equation (4.1) can then be expressed as

$$m\left(\frac{\delta}{\delta t} \dot{\bar{x}} + \bar{\omega}_o \times \bar{x} \right) = \bar{F}_e$$

and in component form

$$m(\dot{u} - v r) = (\bar{F}_e)_x$$

$$m(\dot{v} + u r) = (\bar{F}_e)_y$$

Transformation to landscape coordinates is carried out by

$$\begin{pmatrix} \dot{X} \\ \dot{Y} \\ 0 \end{pmatrix} = A^t \begin{pmatrix} u \\ v \\ 0 \end{pmatrix} = \begin{pmatrix} u \cos \psi - v \sin \psi \\ u \sin \psi + v \cos \psi \\ 0 \end{pmatrix}$$

Here the yaw angle ψ is integrated from the equation

$$I_z \dot{r} = (\bar{M}_e)_z$$

$$\dot{\psi} = r$$

with suitable initial values.

The main problem is to express the external forces $\bar{F}_e$ and moments $\bar{M}_e$ in the state variables used. This will be dealt with in the following sections.

5 EXTERNAL FORCES

The external forces which act upon the vehicle are in this model

1. Tire friction forces and moments

2. Wind forces and moments

The tire friction forces generally are functions

$$F = F(\alpha, S, F_z)$$

The dependance of the vertical load F_z is important and hence a semi-static load transfer is used

$$F_{z1} = F_{zS1} - \frac{h}{2\ell} \cdot (\bar{F}_e)_x - \rho_F \cdot \frac{h}{t_{w12}} \cdot (\bar{F}_e)_y$$

$$F_{z2} = F_{zS2} - \frac{h}{2\ell} \cdot (\bar{F}_e)_x + \rho_F \cdot \frac{h}{t_{w12}} \cdot (\bar{F}_e)_y$$

$$F_{x3} = F_{zS3} + \frac{h}{2\ell} \cdot (\bar{F}_e)_x - \rho_R \cdot \frac{h}{t_{w34}} \cdot (\bar{F}_e)_y$$

$$F_{z4} = F_{zS4} + \frac{h}{2\ell} \cdot (\bar{F}_e)_x + \rho_R \cdot \frac{h}{t_{w34}} \cdot (\bar{F}_e)_y$$

The constants ρ_F and ρ_R decide how the rolling torque is distributed between front and rear axles and correspond to different roll stiffnesses. Further we have the following relationship

$$\rho_R = 1. - \rho_F \qquad 0. < \rho_F < 1.$$

It remains to express α and S in the state variables. The wheel hub velocity is obtained from

$$\dot{\bar{x}}_i = \dot{\bar{x}} + \overline{\omega_o} \times \overline{\rho_i} = \begin{pmatrix} u - \eta_i r \\ v + \xi_i r \\ 0 \end{pmatrix}$$

and this is expressed in the wheel coordinate system by

$$\begin{pmatrix} u_i \\ v_i \\ 0 \end{pmatrix} = B_i \cdot \dot{\bar{x}}_i$$

where

$$B_i = \begin{pmatrix} \cos\delta_i & \sin\delta_i & 0 \\ -\sin\delta_i & \cos\delta_i & 0 \\ 0 & 0 & 1 \end{pmatrix}$$

The slip angle α_i is defined by

$$\alpha_i = \arctan\left(\frac{v_i}{u_i}\right)$$

and the longitudinal slip S_i by

$$S_i = 1 - \frac{R\,\Omega_i}{u_i}$$

where Ω_i is the rotational speed of the wheel, which must be computed by solving the rotational equation of of motion for each wheel. This will be dealt with in a proceeding section.

Thus in principle it is possible to obtain the tire forces and moments from the state variables. These are expressed in the wheel coordinate system and transformed to the vehicle system.

Finally we obtain

$$(\bar{F}_e)_y = \sum_i F_{wiy} + F_{Ly} \qquad (5.2)$$

$$(\bar{F}_e)_x = \sum_i F_{wix} + F_{Lx} \qquad (5.3)$$

$$(\bar{M}_e)_z = \sum_i M_{zi} + \sum_i (\xi_i F_{wiy} - \eta_i F_{wix}) + M_{Lz} \qquad (5.4)$$

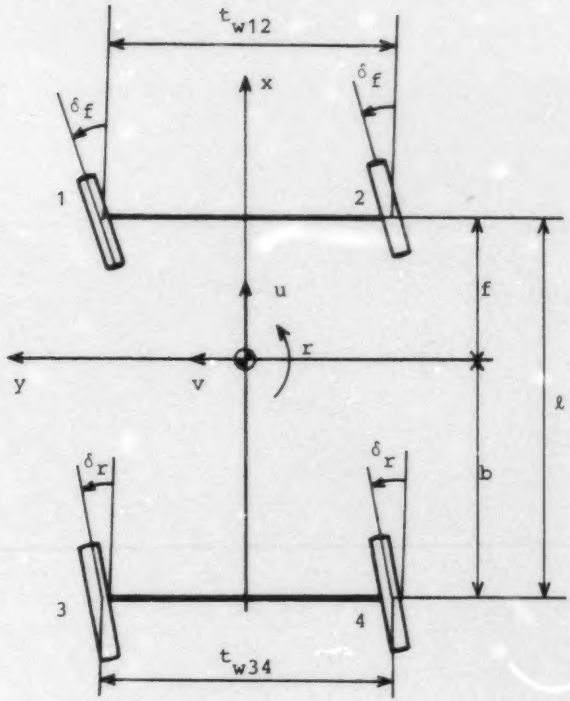

Figure 5.1 Positive directions of steer angles and velocities.
Wheel number indices.

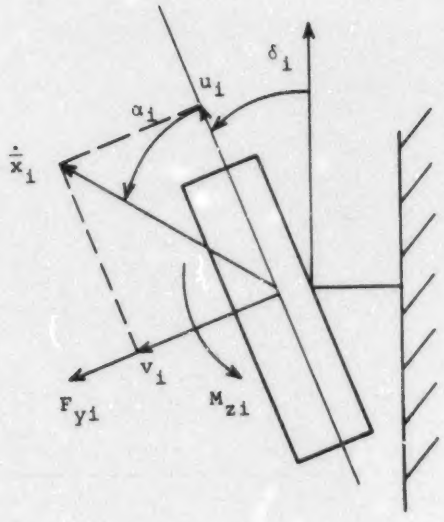

Figure 5.2 Positive directions of steer angle δ_i slip angle α_i and side force F_{yi}

6 WHEEL DYNAMICS

A major problem when simulating rolling vehicles is to integrate the rotational equations of motion. This is due to the behaviour of the reaction force between tyre and road when applying braking or driving torque at the wheel axle. In this section we will concentrate on this problem and calculate the timestep necessary to get an accurate description of the time history. We consider first a rolling wheel according to figure 6.1. The subscript "i" to denote wheel no "i" has been dropped in this section to make the equations more readable.

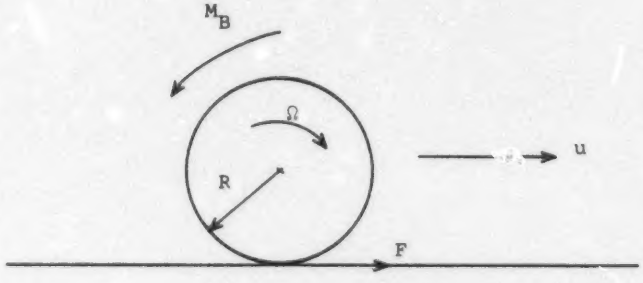

Figure 6.1 Positive directions of forces and speeds in the wheel rotation equations.

The braking torque M_B is applied at the axle O. The reaction force F is a function of the slip S according to the schematic figure 6.2.

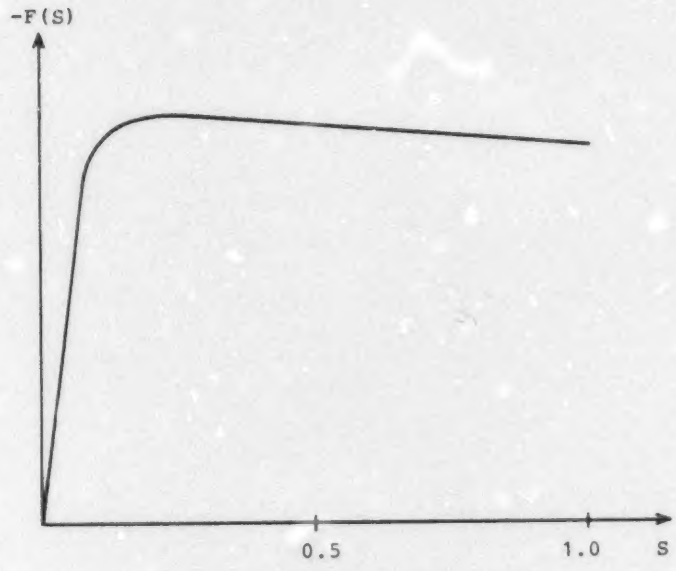

Figure 6.2 Schematic representation of the longitudinal force as a function of slip.

Here the slip is defined by

$$S = 1 - \frac{R \cdot \Omega}{u} \tag{6.1}$$

The rotational equation of motion for the wheel is then

$$I\dot{\Omega} = M_B - R \cdot F(S) \tag{6.2}$$

A change of variables and differentiation of (5.1) give

$$\dot{S} = -\frac{R}{u}\dot{\Omega} + \frac{R\,\Omega}{u^2}\dot{u}$$

We make the simplifying assumption that the change of Ω is large compared to that of u. Then approximately

$$\dot{S} = -\frac{R}{u}\dot{\Omega} \tag{6.3}$$

and (6.3) in (6.2) gives

$$\dot{S} = \frac{R}{uI} (M_B + R \cdot F(S)) \tag{6.4}$$

We simplify further by considering the first order expansion of $F(S)$

$$F(S) = F(S_o) + \frac{dF}{dS} (S_o) \cdot (S - S_o)$$

For each timestep we shall thus solve the initial value problem

$$\begin{cases} \dot{S} = \frac{R}{uI} (M_B + R \cdot F(S_o) + R \frac{dF}{dS}(S_o) \cdot (S - S_o)) \\ S(0) = S_o \end{cases}$$

We simplify the notation by assuming $S_o = 0$ and setting

$$F(S_o) = F$$

$$\frac{dF}{dS}(S_o) = -C_s$$

Then

$$\begin{cases} \dot{S} + \frac{1}{T}S = \frac{1}{T \cdot C_s} \left[\frac{M_B}{R} + F \right] \\ S(0) = 0 \end{cases} \tag{6.5}$$

where

$$T = \frac{I \cdot u}{R^2 \cdot C_s} \tag{6.6}$$

Assuming that C_s, M_B and T are constant during the time-step it is easy to write down the exact solution. However equation (6.5) is actually only a first order

filter with time-constant T. For a passenger car driving at medium speed normal values are

$I = 1\ kgm^2$
$u = 20\ m/s$
$R = 0.3\ m$
$C_s = 60\ 000\ N/unit\ slip$

This will give

$T \approx 4\ ms$

In the simulator the time-step used is actually 20 ms. One could of course use a much shorter time-step in the slip equations but this will increase the total program time, getting it into the neighbourhood of the absolute limit 20 ms.

Very little information is to gain by taking the wheel moment of inertia into account when C_s is high. This is the case in the elastic region of the force-slip curve i.e. for small slip values.

The considerations above have led to the following approach in the simulator program. The slip region is divided into two parts, I and II. See figure 6.3.

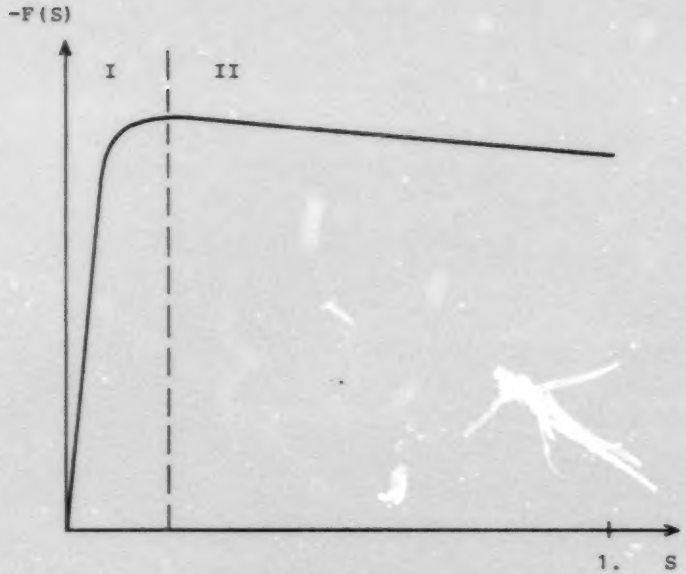

Figure 6.3 Partition of the slip interval into regions I and II with different methods of solving the rotational equation of motion.

It is necessary that $H = -F(S)$ is strictly monotonous in region I thus ensuring the existence of the inverse function H^{-1}.

In region II there might occur two kinds of singularities: $C_s = 0$ and/or $u = 0$. The first case is avoided by Maclaurin-expansion of the solution operator to (6.5) giving the result for small values of C_s.

$$\Delta S = S - S_o = \begin{cases} \frac{1}{C_s}\left(1 - e^{-\frac{\Delta t}{T}}\right)\left(\frac{M_B}{R} + F\right) & |C_s| \geq \varepsilon \\ \frac{R^2 \cdot \Delta t}{I \cdot u}\left(\frac{M_B}{R} + F\right) & |C_s| < \varepsilon \end{cases} \qquad (6.7)$$

In the second case we simply use

$$T = \frac{I \cdot u_o}{R^2 \cdot C_s} \qquad \text{for} \quad u < u_o$$

The strategy is then quite clear. Assume that S_n has been computed. Then if

$S_n \in I$

A: $S_{n+1} = G\left(\frac{M_{B_{n+1}}}{R}\right)$

where G is defined in both I and II by linear extension of H^{-1} into region II

$S_n \in II$

B: $S_{n+1} = S_n + \Delta S$

where ΔS is computed according to (6.7). If then the new $S_{n+1} \in I$ this value is neglected and instead computed according to A.

7 TIRES AND SUSPENSIONS

7.1 Tire model

The applications of the simulator are very gereral. They may vary from normal driving during extended periods to severe manoeuvres on low friction. It is essential that the friction forces during cornering and braking are reproduced as accurately as possible. All these demands point to a fairly complex representation of tire data. Generally the friction forces are functions

$$F_x = F_x\ (\alpha,\ S,\ F_z,\ \gamma)$$

$$F_y = F_y\ (\alpha,\ S,\ F_z,\ \gamma)$$

where

S = longitudinal slip
α = slip angle
F_z = vertical load
γ = camber angle

with a nonlinear dependence on the different variables. There are two possible approaches here. One can try to find analytical expressions with only a few input data, such as cornering stiffness, peak friction valus etc. The most commonly used model of this kind is due to Dugoff et.al. [2] and is described in an earlier VTI- report [10].

This model is able to give a qualitatively and in some respects quantitatively correct description of the complex interaction between longitudinal and lateral forces. The tire forces as well as the aligning torque are given as explicit functions of the slip angle, the longitudinal slip and the vertical load. These

functions are derived from the assumption of a certain distribution (constant and parabolic have been tried) of the vertical load over the contact area. To get a better correspondence with actual tire data the cornering stiffness and the peak lateral friction number may vary as second order polynomials of the vertical load. The coefficients of these polynomials can be directly obtained from the extensive tire investigation performed by Calspan [12].

Theoretical models of this type have been used in the simulator for some time giving good results [8]. However, the coupling between lateral and longitudinal forces seems to be too strong, which will exaggerate over-understeering characteristics for rear and front driven cars respectively. This oversensitivity for traction and braking forces can be seen when comparing tire-data from the Swedish ESV-program [14] with those obtained with Dugoff's equations. In our opinion these analytical expressions must be used very carefully, especially when stability questions arise. They will be very useful as long as qualitative studies are sufficient and program economy is an important matter. It is always possible to model a car with reasonable behaviour using such a simple analytical tire model, but for strict vehicle handling studies something better is needed.

The other approach is to resort to experimentally measured data and interpolate between these. The drawback here is that a very substantial set of data has to be measured and put into the program. These data can also be hard to find, because values for combined cornering and braking are scarce in the literature. Further, the procedure of interpolating between tables describing functions of several variables can be time consuming, which is disadvantageous when working with

a real time program.

Despite this we have found a matrix or tabular formulation worthwhile. Some simplifications have been introduced and our approach is very similar to that in [3].

To avoid dealing with 3- dimensional matrices the following factorizations are assumed

$$F_y(\alpha, S, F_z) = -G_y(F_z, \alpha) \cdot g_{yred}(\alpha, S) \qquad (7.1)$$

$$F_x(\alpha, S, F_z) = -H_x(F_z) \cdot G_x(S) \cdot g_{xred}(S, \alpha) \qquad (7.2)$$

The minus-sign is only a consequence of the sign conventions and a wish to keep the different functions in the right hand sides positive for positive arguments.

All the factors are scalar functions of respective variables. G_y, g_{yred}, g_{xred} and G_x are defined on pointsets where intermediate values are computed by linear interpolation. The g_{xred}, g_{yred} and H_x functions are normalized in the sense that

$$g_{yred}(\alpha, 0) = g_{xred}(S, 0) = 1$$

$$H_x(F_z) = 1 \quad \text{for } F_z = F_{z,\,\text{nominal}}$$

This will in effect mean that $G_y(F_z, \alpha)$ are the side-force - slip angle curves at zero longitudinal force for different forces. Similar arguments are valid for $G_x(S)$.

In the simulator program the following point sets have been used. They are considered to give a reasonable resolution of the actual curves but still are possible to use in real time applications.

$G_y\ (F_z, \alpha)$: (5 x 6)

$g_{yred}\ (\alpha, S)$: (6 x 6)

$G_x\ (S)$: (6)

$g_{xred}\ (S, \alpha)$: (6 x 6)

For the function H_x is assumed a simple linear dependence

$$H_x\ (F_z) = F_z\ /\ F_{z,nominal}$$

The tire force functions are extended to negative values of α and S by

$$F_y\ (-\alpha, S, F_z) = -F_y\ (\alpha, S, F_z)$$

$$F_y\ (\alpha, -S, F_z) = F_y\ (\alpha, S, F_z)$$

$$F_x\ (-\alpha, S, F_z) = F_x\ (\alpha, S, F_z)$$

$$F_x\ (\alpha, -S, F_z) = -F_x\ (\alpha, S, F_z)$$

7.2 Aligning torque. Free rolling wheel

When a free rolling wheel is forced to move at a certain slip angle a reaction force is produced at the contact patch. In the forward, adhesion region no sliding occurs and the force is built up by elastic deformation of tread elements. In the rear, nonadhesion region the friction force limit is reached with sliding as a consequence. This will mean that the resultant is positioned behind the centre of the contact area. This can be expressed as a torque, the aligning torque,

or as a moment arm, the tire caster. We use a simple expression for the aligning torque taken from [13].

$$M_{AZO} = -(K_1 \cdot F_Z + K_2 \cdot |F_y|) \cdot F_y \qquad (7.3)$$

Equation (7.3) is probably the simplest expression that will reproduce the most important qualities of M_{AZ}. This is expected to grow for increasing F_y to a maximum and then decrease to almost zero, when total sliding occurs over the contact area. The term $K_1 \cdot F_2$ represents of course the tire caster or pneumatic trail. The magnitude of K_2 can also be estimated by observing that

$$M_{AZO} \approx 0 \quad \text{for } |F_y| \approx \mu \cdot F_Z$$

which would implicate

$$K_1 \cdot F_Z + K_2 \cdot \mu F_Z = 0$$

$$\therefore K_2 = -K_1/\mu$$

The aligning torque is very important for the handling of the vehicle. A suspension may be designed with a small caster offset. The tire caster must then be added to this to give the total moment arm for the lateral force. Almost all suspensions are fixed to the sprung mass with elastic bushings. The resulting torque from the tire forces may deflect the suspension and add or subtract steering angles. The effect is that the system tire-wheel-suspension may exhibit quite different lateral force-slip angle curves than the tire itself. The handling qualities are a consequence of the balance between the effective cornering coefficients at the front and the rear. The steering system has usually relatively high compliance which is a decisive factor for the under-

steering characteristic of a given vehicle.

It could be enlightening at this point to study the relative importance of these factors. Jaksch has published several reports [6, 7], where first order expressions have been given for the overall compliance. Using his values for Volvo 760 the total compliance at the front axle is composed of the following contributions:

1. The tires: 64%
2. Steering compliance: 31,7%
3. Roll-steer and camber: 4,3%
4. Suspension compliance: 0%

That the influence from suspension compliance is nil depends on the fact that the side force vector has zero moment arm in this special case. The pneumatic trail and the suspension moment arm eliminate each other. However, at larger side forces the pneumatic trail will decrease and then the suspension compliance will have some effect on the total compliance.

With the same argument it will turn out that the steering compliance will contribute less at higher sideforces. In this region nonlinear effects will tend to play a role. The vertical load sensitivity of the tires is most important of these. The use of a stiff roll stabilizer at the front is a deliberate step of the vehicle designer to increase the understeering tendency especially at the limit.

7.3 Suspension and steering compliances. Effective cornering characteristics

A simple way to account for the compliances in the steering system and the suspensions is to couple them to the tire characteristics. This has the same effect as connecting a number of springs in series. We follow the same procedure here as outlined by Pacejka in [11].

Let us consider a wheel that is suspended according to figure 7.1. The slip angle of the wheel-suspension system is α_V (angle between speed vector and longitudinal direction of chassis), while the slip angle of the tire is α. The induced angle due to elasticity is denoted by α'.

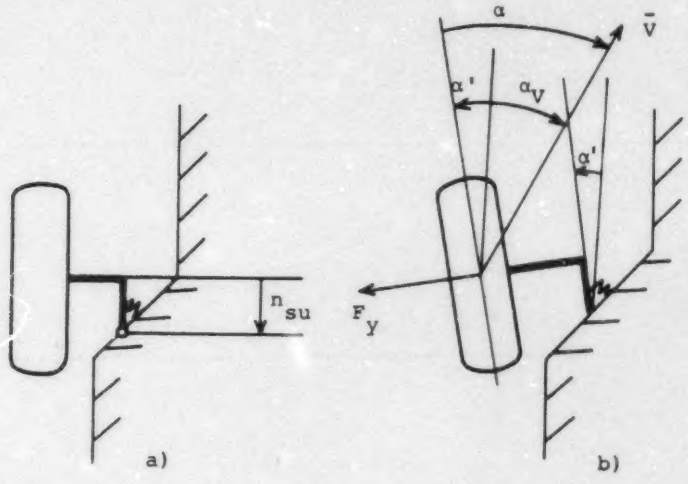

Figure 7.1 Effect of suspension compliance.
a) Straight driving
b) Wheel working in direction defined by $\bar{v}$

Then

$$\alpha = \alpha_y + \alpha'$$

where

$$\alpha' = F_y \cdot n_{su} \cdot C_{su}$$

If we also consider the change in position of F_y due to the pneumatic trail Δ

$$\alpha' = F_y \cdot n_{su} \cdot C_{su} - F_y \cdot \Delta \cdot C_{su}$$

where Δ is obtained from (7.3)

$$\Delta = M_{AZO}/F_y$$

Exactly the same reasoning can be carried out for the steering compliance. The moment arm is then defined by the caster offset and the pneumatic trail. The steering axis is denoted by 0 and is fixed in the suspension arms, which in turn will flex the angle α''. Then

$$\alpha'' = -(n_c + \Delta)\ F_y \cdot C_{st}$$

where the steering compliance C_{st} is measured around the point 0.

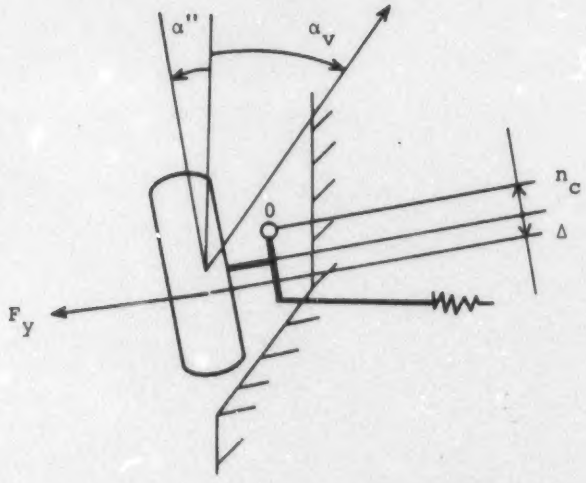

Figure 7.2 Effect of steering system compliance

Finally

$$\alpha = \alpha_v + \alpha' + \alpha'' =$$

$$= \alpha_v + F_y \cdot [n_{su} \cdot C_{su} - n_c C_{st} -$$

$$- \Delta \cdot (C_{su} + C_{st})] \qquad (7.4)$$

The effective cornering characteristic is now computed by a shift in the $F_y - \alpha$ curve. For given F_y we have from (7.4).

$$\alpha_v = \alpha + G(F_y)$$

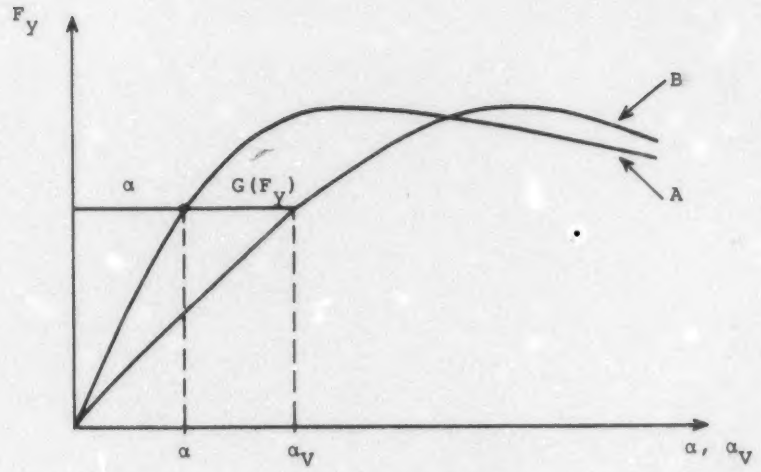

Figure 7.3 Construction of effective cornering characteristics

A: Tire characteristics

B: Tire-suspension characteristics due to different compliances

7.4 Tire carcass elasticity

In the previous section we pointed out the importance of the aligning torque for the handling qualities. However, the expression (7.3) is only valid for a free-rolling wheel with only lateral force applied. When traction and/or braking forces also exist the contact area will be displaced due to carcass elasticity. This effect is not neglectable and is one of the reasons for the tendency of a vehicle to tuck inwards when the throttle is released in a curve. The explanation for this is quite simple according to figure 7.4.

The formulation here follows Pacejka [3, p. 794 - 798] but is simplified by neglecting the vertical torsional compliance of the tire.

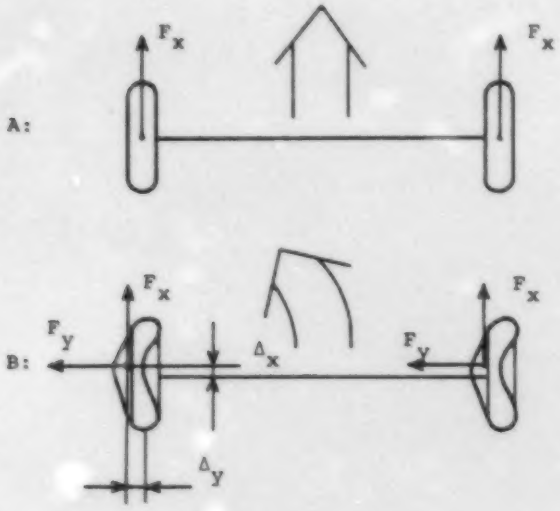

Figure 7.4 Displacements of contact area due to carcass elasticity.
A: Straight driving
B: Cornering

From the figure it is clear that both F_x and F_y will produce torques with moment arms Δ_y and Δ_x respectively. Introducing the tire compliances C_{tx} and C_{ty} in each direction we obtain for the aligning torque (one wheel only)

$$M_{AZ} = M_{AZO} - F_x \cdot \Delta_y + F_y \cdot \Delta_x =$$

$$= M_{AZO} - F_x \cdot F_y \cdot C_{ty} + F_y \cdot F_x \cdot C_{tx} =$$

$$= M_{AZO} + F_x \cdot F_y (C_{tx} - C_{ty}) \qquad (7.5)$$

Since C_{tx} normally is less than C_{ty} the effect of traction forces is understeering both for front and rear driven cars. It is also quite clear that the changed torques can induce steering angles due to compliances. These are taken care of by assuming proportionality to the correction term in (7.5). Thus

$$\Delta\delta = F_x \cdot F_y \, (C_{tx} - C_{ty}) \, C_M \qquad (7.6)$$

C_M is here the total compliance of the suspension and steering system per wheel.

8 BRAKING SYSTEM

The braking torque applied at each wheel is in principle proportional to the signal from a transducer in the hydraulic braking system which in part is retained in the cabin from the original passenger car. No attempt has been made to model time delays but the option of a pressure reduction valve to the rear wheels exists. The force at the brake pedal B_{ped} is transformed into line pressures P_f to the front and P_r to the rear according to figure 8.1

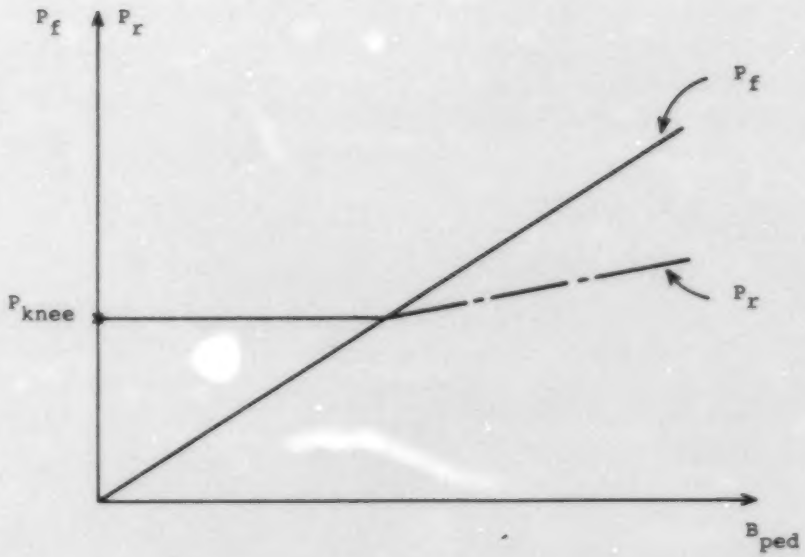

Figure 8.1 Diagram showing effect of line pressure reduction valve to rear wheels

The equations for the line pressures are as follows:

$$P_f = B_{ped} \cdot BRC_1$$

$$P_r = \begin{cases} B_{ped} \cdot BRC1; & P_r \leq P_{knee} \\ P_{knee} + BRC2 \cdot (B_{ped} - \frac{P_{knee}}{BRC1}); & P_r > P_{knee} \end{cases}$$

These pressures are multiplied with constants to give the braking torque at each individual wheel

$$M_{Bi} = P_f \cdot BRT_i \qquad i = 1,2$$

$$M_{Bi} = P_r \cdot BRT_i \qquad i = 3,4$$

Uneven brake distributions can thus be simulated by changing the constants BRT_i.

9 ENGINE AND DRIVE LINE

The engine characteristics are described by torque (M_E) - engine speed (Ω_E) curves for different throttle positions. The used curves are depicted in figure 9.1 and they are constructed in the following way. The throttle position is determined by the normalized variable X_E ($1 \geq X_E \geq 0$), where $X_E = 1$ means no throttle and $X_E = 0$ full throttle. Starting from the torque-engine speed curve

$$M_E = f(\Omega_E); \; X_E = 0$$

for full throttle, the curves for $X_E \neq 0$ are computed by the following equations:

$$\Omega' = \Omega_L + \Omega_{EC} \cdot X_E^2$$

$$M_E = f(\Omega') - M_{EC} \cdot X_E^2$$

Essentially this is a translation along a straight line of the curve for $X_E = 0$ and the meaning of Ω_{EC} and M_{EC} is clear from figure 9.1. This algorithm gives a good fit to experimental "performance fields" and a natural feel of the engine when driving the simulator while still fulfilling the demand of short computation time.

The engine model has also been validated by Godthelp et al [5] using an instrumented car. By suitable choice of the parameters M_{EC} and Ω_{EC} it has been possible to obtain good correspondence between measured values and those predicted by the model.

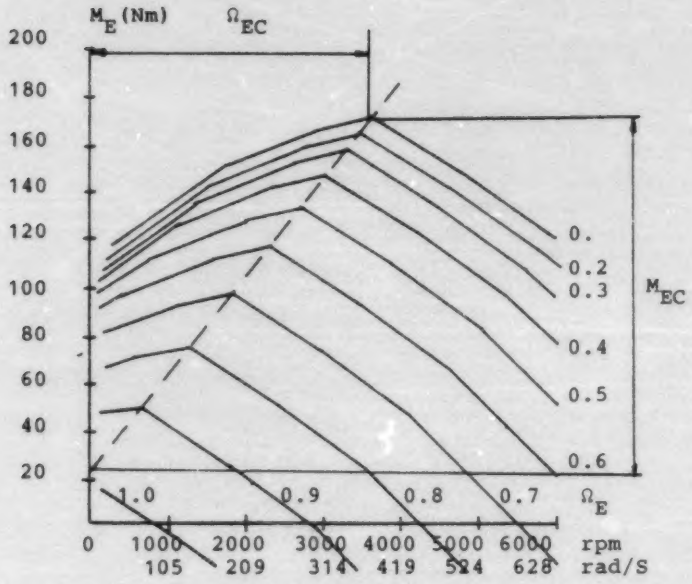

Figure 9.1 Engine torque versus rotational speed for different throttle positions

The rest of the driveline is separated in different blocks.

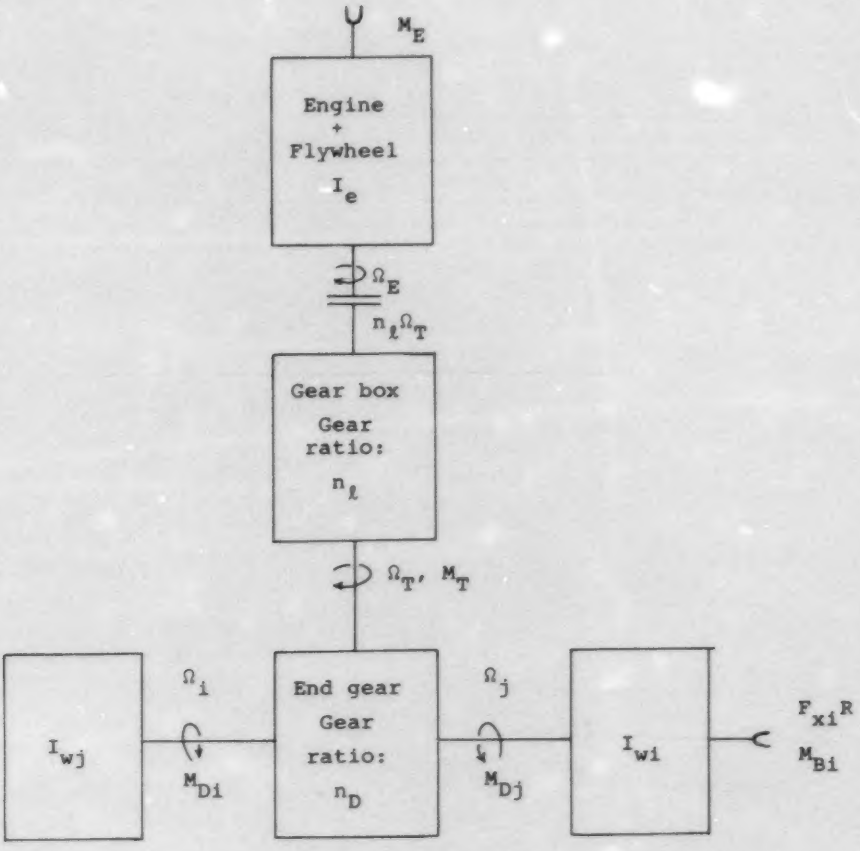

Figure 9.2 Driveline with engine gearbox, end gear and wheels

For the wheels the following equations are valid

$$\begin{cases} I_{wi}\,\dot{\Omega}_i = M_{Di} - M_{Bi} - F_{xi}\cdot R \\ I_{wj}\,\dot{\Omega}_j = M_{Dj} - M_{Bj} - F_{xj}\cdot R \end{cases} \tag{9.1}$$

The end gear has the property of distributing the torque from the driveshaft in equal ratio

$$\begin{cases} M_{Di} = M_{Dj} = \frac{1}{2} n_D \cdot M_T & (9.2) \\ \Omega_T = \frac{1}{2} n_D\,(\Omega_i + \Omega_j) & (9.3) \end{cases}$$

The engine has the following equation of motion

$$I_E\,\dot{\Omega}_E = M_E - M_{Cl} \tag{9.4}$$

and for the gear box the following relations are valid when the clutch is closed

$$M_{Cl} = \frac{1}{n_\ell}\cdot M_T \tag{9.5}$$

$$\Omega_E = \frac{1}{n_\ell}\,\Omega_T \tag{9.6}$$

Elimination between equations (9.1) - (9.6) will give for wheel i

$$(I_{wi} + \tfrac{1}{4} n_D^2 \cdot n_\ell^2 \cdot I_E)\,\dot{\Omega}_i + \tfrac{1}{4} n_D^2 \cdot n_\ell^2 \cdot I_E \dot{\Omega}_j =$$

$$= -M_{Bi} - F_{xi}\cdot R + \tfrac{1}{2}\, n_D \cdot n_\ell \cdot M_E \tag{9.7}$$

and a similar expression (9.8) for the other wheel. The rotations of the wheels are coupled by the engine-flywheel moment of inertia.

Numerically it has proved to be difficult to solve the equations (9.7-8). Instability has occurred when

considering the $\dot{\Omega}_j$-term as a torque in the right hand side of (9.7). This is probably due to the long time-step used and the fact that the coefficient matrix of $(\dot{\Omega}_i, \dot{\Omega}_j)$ has a determinant near zero making the system (9.7) and (9.8) sensitive to disturbances. The question needs further clarification but this is not carried out in this context.

To avoid the difficulty we have chosen to decouple the equations (9.7) - (9.8) by exchanging the coupling term $\dot{\Omega}_j$ for $\dot{\Omega}_i$ in (9.7) and similarly in (9.8).

The equations are then easy to solve using the procedure outlined earlier. In the program the drive shaft speed Ω_T is then determined by (9.3). In this way the main results of the differential are retained and are in fact correct when the wheels move synchronously.

10 STEERING SYSTEM

In the preceding chapters we have given a complete description of the dynamics of the vehicle in the sense that the motion of the vehicle is determined if the initial conditions and certain control variables are specified. These variables are controlled by the driver and are as follows:

1. Angle of steering wheel
2. Brake
3. Throttle
4. Gear
5. Clutch

The steer angle is transmitted from the steering wheel to the front wheels via the steering system. It is a well-known fact that the driver receives a lot of information concerning the road and the manœuvre ("road feeling") from the reaction torque at the steering wheel. This feedback mechanism is thus important to model rather carefully. Most parts of this have already been presented in this report. The aligning torque as well as the tire forces were introduced in section 7 and the compliance of the steering system has already been included in the tire data. The resulting torque at the tires is then transmitted to the steering wheel through the steering gear with ratio n_s. Some damping and friction forces are also included. Most of the expressions used are linear for simplicity but more complex representations are possible if the need would arise. We use mainly equations derived in [9, p. 439] for the effects of caster and king pin offsets. The derivation is rather lengthy and the reader is referred to [9] for all details. We have chosen to consider the case that the braking and tractive torques are taken up by the steering axis

rather than by a drive-shaft coupled to the engine.

Due to the orientation of the steering axis the tire forces will create a torque at the steering wheel. The steering axis is inclined and situated at a certain distance from the wheel plane. These angles and distances are defined in figure 10.1.

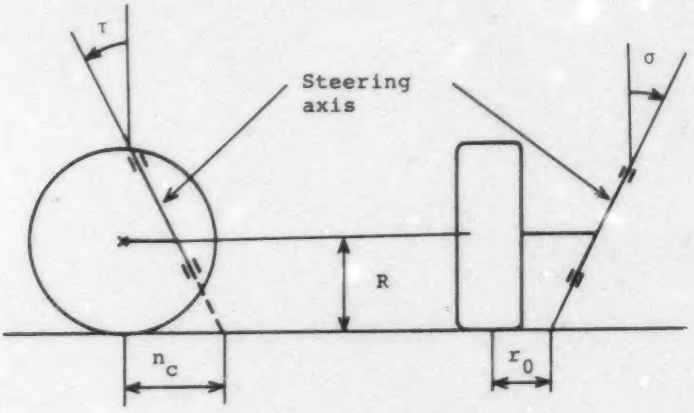

Figure 10.1 Front wheel seen from the side and from the rear.

τ = caster angle
n_c = caster offset
δ = king pin inclination
r_0 = king pin offset

It is now possible to express the combined torque M_R from both sides assuming that the geometrical data are the same for both sides. Then, for small steer angle δ

$$M_R = (F_{x2} - F_{x1})\cdot r_0 - (F_{y1} + F_{y2})\cdot n_c + (F_{z2} - F_{z1})\cdot a_1 + (F_{x1} + F_{x2})\cdot\delta\cdot a_2 + (F_{y2} - F_{y1})\cdot\delta\cdot a_3 - (F_{z1} + F_{z2})\cdot\delta\cdot a_4 + M_{AZ1} + M_{AZ2}$$

where

$$a_1 = r_0 \tan\tau + n_c \tan\sigma$$

$$a_2 = \tan\sigma \cdot (r_0' \tan\tau + n_0 \tan\sigma)$$

$$a_3 = r_0' \tan^2\tau + n_0 \tan\tau \tan\sigma + R \cdot \tan\sigma$$

$$a_4 = r_0' \tan\sigma - n_c \tan\tau$$

with

$$r_0' = r_0 + R \cdot \tan\sigma$$

$$n_0 = n_c - R \cdot \tan\tau$$

and M_{AZ1}, M_{AZ2} are the complete expressions for the aligning torques as given in section 7.4.

Some damping is also included in the system. This has mainly the form of Coulomb friction to give hysteresis effects. See figure 10.2

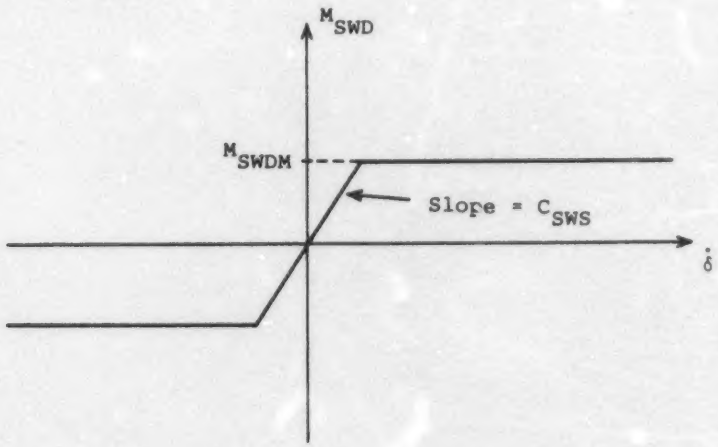

Figure 10.2 Damping in steering system

The friction function is defined by

$$M_{SWD} = \begin{cases} C_{SWS} \cdot \dot{\delta}_{SW} & |M_{SWD}| \leq M_{SWDM} \\ M_{SWDM} \cdot \text{sign}\ (\dot{\delta}_{SW}) & \text{otherwise} \end{cases}$$

M_{SWD} is then passed through a first order filter with time constant τ_{SW} to get a smoother function.

Finally, we obtain for the reaction torque at the steering wheel

$$M_{SW} = \left(-\frac{1}{n_s} \cdot M_R + \tilde{M}_{SWD} \right) C_{servo}$$

where

$\tilde{M}_{SWD}$ = filtered Coulomb damping

C_{servo} = function to reduce overall torque to simulate servo-assisted steering system

n_s = steering ratio

11 ROLLING RESISTANCE AND WIND FORCES

A free rolling vehicle on a flat surface will finally come to a stop. This is due to the so called rolling resistance and air resistance. At low speeds the former effect dominates, at high speeds the latter. Figure 11.1 from [1] will show this clearly.

It can be seen that the rolling resistance is almost constant over most of the range while the air resistance has a parabolic shape as a function of velocity.

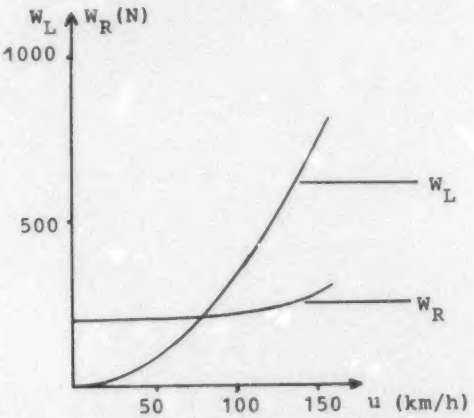

Figure 11.1 Comparison between effects of rolling resistance W_R and aerodynamic drag W_L for a typical passenger car [1].

The rolling resistance is mainly due to hysteresis effects when the tire compresses and expands. It is proportional to the vertical load and added to the braking torque of each wheel. We have chosen to include rolling resistance at each wheel rather than as a force in the centre of gravity. The reason for this is that the rolling resistance will to some extent contribute to the understeering of a given vehicle if applied at each wheel. This might affect the handling qualities at least in extremum.

Thus we add a term

$$R \cdot C_R \cdot F_{zi}$$

to the braking torque M_{Bi} at each wheel.

Air resistance is given by

$$F_{Lx} = -C_w \cdot u^2$$

where

$$C_w = 0{,}5 \cdot C_{Ax} \cdot \rho_A \cdot A_0$$

In some applications it can be interesting to introduce some surprise elements to the driver. One attempt in that direction is the effects of wind gusts and side wind.

For simplicity we have only considered side wind perpendicular to the vehicle trajectory and small aerodynamic side slip angle β_A. These results are directly taken from Mitschke [9, p. 98-101].

$$F_{Ly} = d_{w1} \cdot v_w \cdot u \qquad (11.1)$$

$$M_{Lz0} = d_{w2} \cdot v_w \cdot u \qquad (11.2)$$

that is, both the lateral force and the yawing moment from the sidewind are directly proportional to the ambient wind velocity v_w and vehicle speed u. The coefficients d_{w1} and d_{w2} can be expressed in more conventional aerodynamic terms

$$d_{w1} = \frac{C_{Ay}}{\beta_A} \cdot A_0 \cdot \frac{\rho_A}{2}$$

$$d_{w2} = \frac{C_{AMz}}{\beta_A} \cdot \ell \cdot A_0 \cdot \frac{\rho_A}{2}$$

Experimentally it has been found that the side force coefficient C_{Ay} and the yawing moment coefficient C_{AMz} in this case are linear functions of β_A. This justifies considering d_{w1} and d_{w2} as constants.

It should further be observed that the aerodynamic forces as given by (11.1) and (11.2) are conventionally related to a point half between the axles rather than the centre of gravity. For use in equation (5.4) we thus obtain

$$M_{Lz} = M_{Lz0} - F_{Ly}(\ell/2 - \xi_1) =$$

$$= [d_{w2} - d_{w1}(\ell/2 - \xi_1)]v_w \cdot u$$

12 VALIDATION

A most important aspect of computer simulation is validation of the model. Comparisons with field tests must be made to establish the limits of the model and under what circumstances the results can be relied upon. The difficulties here are several.

One must have correct input data to the program which can be very hard to obtain. Several of the data used in the model here are not generally available. We have stressed the importance of the balance between effective cornering characteristics of the front and rear axles. These are depending on the tire itself and the suspension steering compliances, both of which unfortunately are among the hardest data to get.

Further the model itself can be erronous in the sense that certain factors, which might be important, have been neglected when putting the mathematical model together. Everything can for natural reasons not be included and the final result reflects the assessments or perhaps prejudices of the constructor of the model. Certainly there is also a risk for undetected programming errors especially for very complex models leading to large programs.

The possibility of actually driving the mathematical model in the simulator is a severe test indeed. Many errors have been found this way and it has also deeply influenced the current model.

The computer program for the vehicle dynamics has been used separately for more conventional, digital simulations. The evaluation then concentrates on the behaviour of the vehicle during single lane changes with different amplitudes and frequencies. The test procedure is based on a draft proposal from ISO TC 22 SC9 [15].

The forward speed is 80 km/h when driving at a straight course on dry asphalt and then the steering wheel angle is turned one period of a sine wave. The amplitude is increased in steps until the stability limit of the vehicle is reached. This is carried out at the frequency 0,5 Hz. The resulting lateral acceleration and yaw velocity will get a first and a second peak. The time lags for these peaks in relation to the steering wheel angle are computed with cross-correlation between the signals and plotted as a function of the first peak of the lateral acceleration. This is of course only a part of the complete test but will give a good indication of the validity of the model.

This approach was used in [8] where an earlier model was shown to give fairly good agreement with results from field tests. At least it was possible to obtain vehicle behaviour ranging from pronounced understeer to oversteer covering the range of normal passenger cars. The main variable here was a reduction factor of cornering stiffness at the front which could be adapted to give an expected result.

In the model in this report we have tried to relate all indata to specified physical properties of the vehicle and in that sense get a more valid model. We have studied an ISO-lane change for a passenger car which has fairly well documented vehicle data as well as field test results.

The correspondence between simulation results and field tests is very good which can be seen in figures 12.1 - 12.2. The only exception is the time lag between lateral acceleration (second peak) and steering angle for high lateral accelerations. This is probably due to lack of accurate tire data. The cornering stiffness is correct for small slip angles while the real tire can utilize

a higher friction number in the sliding region than is assumed in the model. We have also compared the torque at the steering wheel during the lane change at an acceleration level of 5.5 g. The agreement is good (figure 12.3) but it must be pointed out here that some adaption of model parameters has been used, since data for the steering system were less well known.

As a final conclusion it can be stated that the mathematical model used in the driving simulator has shown to be able to predict correctly the transient performance of passenger cars under severe manoeuvres as well as providing a vehicle that feels natural during more normal driving circumstances.

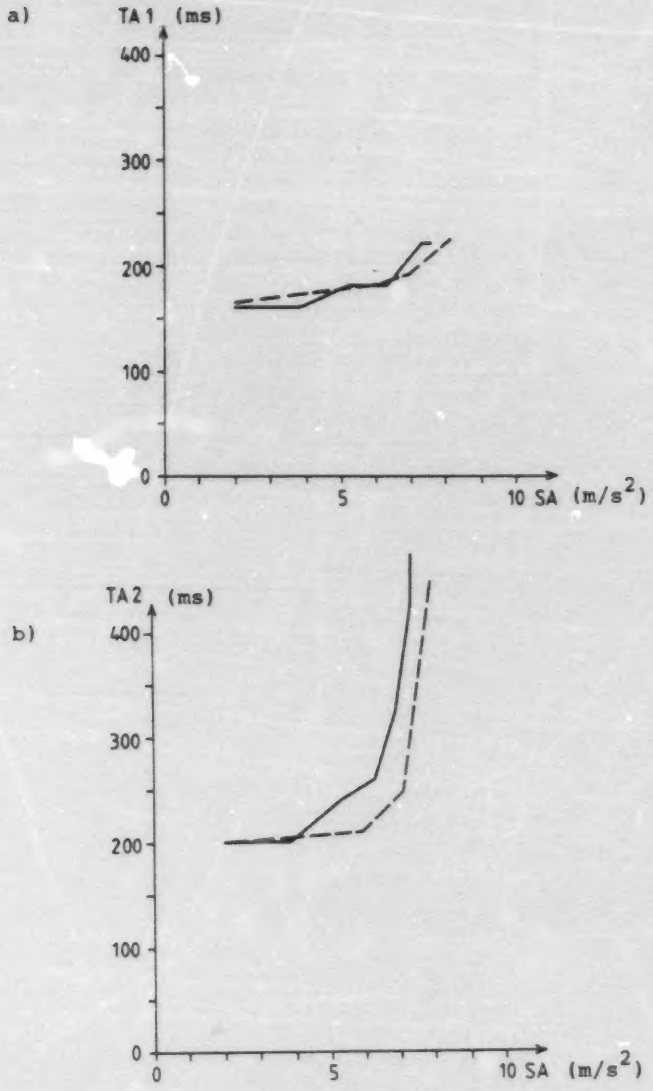

Figure 12.1 Timelag between lateral acceleration and steering wheel angle.
a) First peak b) Second peak
---- Field test
—— Simulation

a)

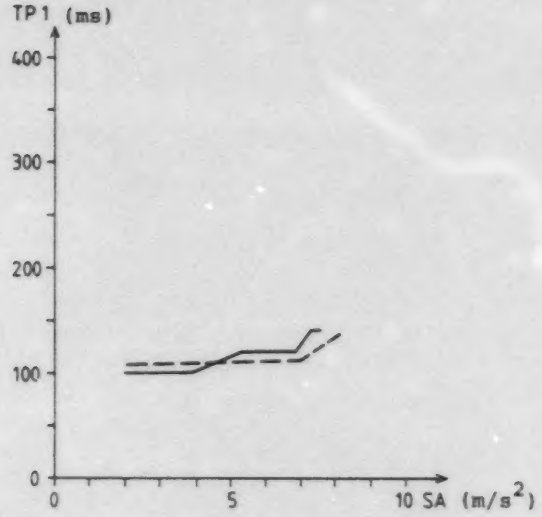

b)

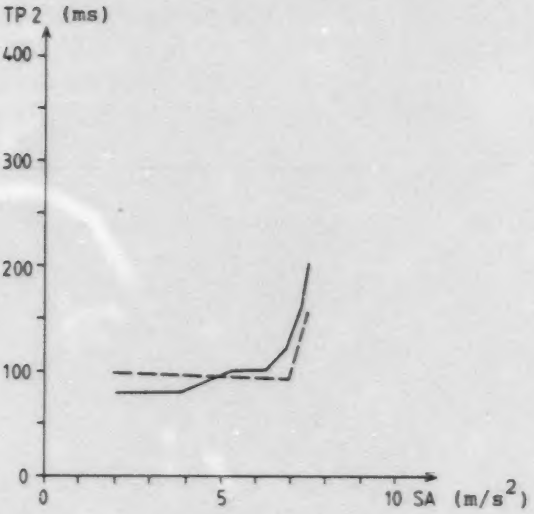

Figure 12.2 Timelag between yaw velocity and steering wheel angle.
a) First peak b) Second peak
---- Field test
—— Simulation

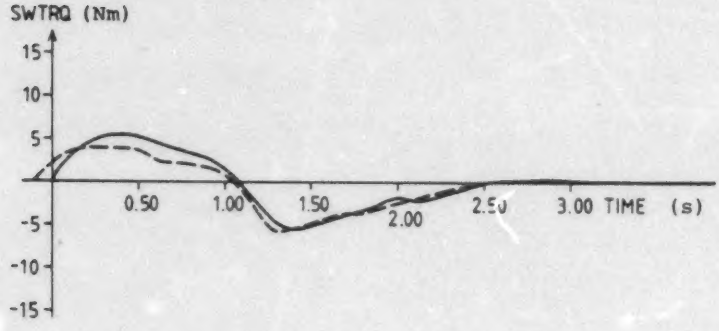

Figure 12.3 Measured and simulated torque at the steering wheel. Lateral acceleration 5.5 m/s^2.
---- Field test
—— Simulation

REFERENCES

1 Barth, R. (1966): Luftkräfte am Kraftfahrzeug. Deutsche Kraftfahrtforschung und Strassenverkehrstechnik, Heft 184.

2 Dugoff, H., Fancher, O.S. & Segel, L. (1969): Tire Performance Characteristics Affecting Vehicle Response to Steering and Braking Control Inputs, Contract No. CTS-460, National Bureau of Standards.

3 Clark, S.K. Ed. (1971): Mechanics of Pneumatic Tires. National Bureau of Standards Monograph 122.

4 Gillespie, T.D., Mac Adam, C.C. & Hu, G.T. (1980): Truck and Tractor-Trailer Dynamic Response Simulation - T3 DRS:V1, Users Manuel. FHWA-RD-79-125.

5 Godthelp, J., Blaauw, G.J. & van der Horst, A.R.A. (1982): Instrumented car and driving simulation: Measurements of vehicle dynamics. Institute for Perception TNO, Soesterberg, Report IZF 1982-37.

6 Jaksch, F.O. (1980): The Steering Characteristics of the Volvo Concept Car. VIIIth ESV Conference Wolfsburg, October 1980.

7 Jaksch, F.O. (1983): Vehicle parameter influence on steering control characteristics, Int. J. of Vehicle Design, vol. 4, no. 2, pp. 171-194.

8 Lidström, M, Nordmark, S & Nordström, O (1981): Handling research in a driving simulator. Computer simulation in real time. Proc. 7th IAVSD-Symposium, Cambridge, UK, September 7-11, 1981.

9 Mitschke, M. (1972): Dynamik der Kraftfahrzeuge, Springer Verlag

10 Nordmark, S. (1976): Development of a driving simulator. Mathematical vehicle model. (In Swedish). National Swedish Road and Traffic Research Institute, Internal report no. 4

11 Pacejka, H.B. (1978): Tyre Factors and Vehicle Handling. Delft Univ. of Technology. WTHD 108.

12 Richter, Bernd (1974): Driving Simulator Studies - The Influence of Vehicle Parameters on Safety in Critical Situations. SAE-paper 74 1105

13 Schuring, D.J. (1976): Tire Parameter Determination. NHTSA PB-263440

14 Nordström, O., Nilsson, A. & Nilsson, B. (1974): Measurements Tyre-Road Characteristics, Swedish ESV program. Report 6-01.

15 ISO TC22 SC9 (Sweden) (1978): Draft Proposal for an International Standard, Road Vehicles - Transient Response Test Procedure. (N 138 rev 1).

LIST OF SYMBOLS

A	Transformation matrix for yaw angle
A_0	Projected frontal area of vehicle
b	Distance centre of gravity - rear axle
B_{ped}	Pedal force (brakes)
B_i	Transformation matrix for steer angle
BRC1	Line pressure - pedal force gradient
BRC2	Line pressure - pedal force gradient after reduction value
BRT_i	Brake torque - line pressure ratio at wheel "i"
C_{AMz}	Aerodynamic yawing moment coefficient
C_{Ax}	Aerodynamic longitudinal force coefficient
C_{Ay}	Aerodynamic side force coefficient
C_M	Total compliance around vertical axis per wheel
C_R	Rolling resistance coefficient
C_s	Braking (driving) stiffness of tire
C_{servo}	Reduction coefficient for steering wheel torque due to servo aid
C_{st}	Steering compliance around vertical axis (one wheel)
C_{su}	Suspension compliance around a vertical axis
C_{SWS}	Viscous damping coefficient for small steering wheel velocities
C_{tx}	Tire deflection - longitudinal force ratio
C_{ty}	Tire deflection - lateral force ratio
C_w	Constant for the aerodynamic drag
d_{w1}	Constant in side wind force equation
d_{w2}	Constant in side wind yawing torque equation
f	Distance between centre of gravity and front axle

F	Tire force
$\bar{F}_e$	Sum of external forces acting on vehicle
F_{Lx} F_{Ly}	Components of aerodynamic forces
$\bar{F}_{wi}$	Tire force vector, wheel "i"
F_{wix} F_{wiy}	Components of tire force vector in vehicle system
F_x	Longitudinal component of tire force in wheel system
F_{xi}	Longitudinal component of tire force in wheel system. Wheel "i"
F_y	Lateral component of tire force in wheel system
F_{yi}	Lateral component of tire force in wheel system. Wheel "i"
$F_{sz1} - F_{sz4}$	Static vertical load on tire 1-4
F_z	Vertical load on tire
$F_{z1} - F_{z4}$	Vertical load on tire 1-4
$F_{2,\ nominal}$	Nominal vertical load of tire
G_x	Longitudinal force - slip at nominal vertical load
g_{xred}	Reduction factor of longitudinal force due to slip angle
G_y	Lateral force - slip angle and vertical load
g_{yred}	Reduction factor of lateral force due to slip
h	Centre of gravity height
H_x	Reduction factor of longitudinal force due to vertical load
I	Moment of inertia of wheel
I_E	Moment of inertia of engine rotating parts plus flywheel
I_{wi}	Moment of inertia of wheel "i"

I_z	Moment of inertia of vehicle around vertical axle through centre of gravity
K_1, K_2	Constants in expression for aligning torque
l	Wheelbase
m	Vehicle mass
M_{AZ}	Aligning torque including carcass elasticity effects (one wheel)
M_{AZ0}	Aligning torque excluding carcass elasticity effects (one wheel)
M_B	Braking torque
M_{Bi}	Braking torque. Wheel "i"
M_{Cl}	Torque transmitted by clutch
M_{Di}	Driving torque. Wheel "i"
M_E	Engine torque
$\bar{M}_e$	Total external torque at vehicle c.g.
M_{LZ}	Yawing torque due to aerodynamic effects
M_R	Reaction torque in steering system
M_{SW}	Reaction torque at steering wheel
M_{SWD}	Maximum Coulomb friction torque in steering system
M_{Zi}	Aligning torque. Wheel "i"
n_c	Caster offset
n_D	End gear ratio
n_ℓ	Gear ratio
n_s	Steering ratio
n_{su}	Moment arm for lateral tire forces acting on suspension
P_f	Line pressure at front brakes
P_{knee}	Line pressure when reduction valve begins to work
P_r	Line pressure at rear brakes

r	Yaw velocity
R	Wheel rolling radius
r_0	Kingpin offset
S	Longitudinal slip
S_i	Longitudinal slip. Wheel "i"
S_n	Longitudinal slip at time $n \cdot \Delta t$
t_{w12}	Wheel track front
t_{w34}	Wheel track rear
u	Longitudinal speed
u_o	Fixed minimal speed in certain expressions to avoid singularities
u_i	Longitudinal speed of wheel "i" in wheel co-ordinate system
v	Lateral speed
v_i	Lateral speed of wheel "i" in wheel coordinate system
v_w	Sidewind velocity
$\bar{x}$	Vector defining position of centre of gravity
X	Landscape coordinate
X_E	Variable defining amount of throttle
Y	Landscape coordinate
α	Slip angle
α'	Steer angle due to suspension compliance
α''	Steer angle due to steering compliance
α_i	Slip angle. Wheel "i"
α_v	Slip angle of vehicle at wheel position
β_A	Aerodynamic sideslip angle
γ	Camber angle
δ_f	Steering angle front

δ_i	Steering angle. Wheel "i"
δ_r	Steering angle rear
δ_{SW}	Steering wheel angle
Δ	Pneumatic trail
Δs	Change in slip during time Δt
Δt	Timestep in integrations
$\Delta x, \Delta y$	Longitudinal and lateral displacements of tire contact patch due to carcass elasticity
$\Delta\delta$	Change in steering angle due to carcass elasticity
ϵ	Fixed small positive number
η_i	y-coordinate of wheel "i"
μ	Peak friction number
ξ_i	x-coordinate of wheel "i"
ρ_A	Density of air
ρ_F	Proportion of rolling torque on front axle
ρ_R	Proportion of rolling torque on rear axle
σ	Kingpin inclination
τ	Caster angle
τ_{SW}	Time constant in first order filter for Coulomb friction in steering system
ψ	Yaw angle
Ω	Wheel rotational speed
Ω_E	Engine rotational speed
Ω_{EC}	Engine rotational speed at maximal torque with full throttle
Ω_i	Rotational speed of wheel "i"
Ω_T	Rotational speed of driveshaft between gearbox and end gear
$\bar{\omega}_0$	Vehicle rotational speed